A Review on Detection of Vein Pattern in Human Body for the Biometric Applications

V. Goutham[1(✉)], D. L. Lakshmi[1], M. K. Hamsashree[1], B. Naveen[1], and D. L. Girijamba[2]

[1] BGSIT, Adichunchanagiri University [ACU], BG Nagara, Karnataka, India
gouthamv77@gmail.com, lakshmidl.ec@gmail.com
[2] Vidyavardhaka College of Engineering, Mysuru, Karnataka, India

Abstract. In the present day scenario, there is huge scope for security systems, medicine. Since, many of the other biometrics systems fails due to one or the other reason, but this veins authentication will be more secured. In this field, the use of veins will be the most secured biometric application for identifying the person or for authentication as the vein patterns will be unique and mainly it is an internal part of the Human body. Also detection of veins is necessary for many medical applications. There are many dieses, which are caused due to disorders in veins and many dieses are cured by operating veins. Vein structure for each human is different and unique. Detection of the vein pattern for many applications will be the key. So, the detection is of high priority and next comes the processing.

Keywords: Veins · Biometrics · Securitysystem · Medicine · Authentication

1 Introduction

The patterns of veins are studied for the application in two different domains. One is for biometrics and another is medical field. In biometrics and authentication, there are different modalities based on the human parts considered and in medical filed it is used to cure many diseases and disorders caused due to the veins.

In biometrics it is used to identify specific person based on behavioural and physiological characteristics. Fingerprints were used for authentication, and later face, palm and iris were used for security purpose as they all unique in every human. These all are extrinsic which are in visible spectrum, which can be misused as these are susceptible for spoof attacking. To overcome the flaws, there was an exposure for intrinsic spectrum like finger veins, palm veins and hand veins. As these veins are soft tubes which are thin walled which carry blood and studies have proved that the pattern of veins are unique in every human.

The challenging part of the biometrics and medical applications is the capturing and processing of vein images. So, capturing of vein pattern is not simple as capturing of face, thumb and iris images, as these were visible parts. So the major part of the vein processing is capturing the vein pattern. It is very difficult to capture the vein pattern as this is the internal part of the human body, which cannot be seen with naked eye. There

D. S. Guru et al. (Eds.): ICCR 2021, CCIS 1697, pp. 1–17, 2022.
https://doi.org/10.1007/978-3-031-22405-8_1

are many constraints in capturing the images of patterns of veins. The very important thing in capturing the vein pattern is Camera.

2 Literature Review

[1] Sarah Hachemi Benziane, Abdelkader Benyettou in their work of an innovative technique was proposed for the extraction of physiological features of dorsal hand vein for the biometric application. Used the dorsal hand near infrared built database and using the different matching features like SAB'11, SAB'13 and NCUT Benchmark. The extraction of required feature for getting efficient results was obtained with the features required which was used in biometric application for person authentication/identification.

[2] Huafeng Qin, Xiping He, Xingyan Yao, Hongbing Li, in their work, in the applications of finger vein detection and in biometric system, may get affected by factors like noise, shadowing which reduces the accuracy. So a novel technique to extract the veins of the finger which detects the structures like valley by curvatures in Radon space. The patterns of veins are enhanced by curvatures values of the valley accordingly.

[3] Yuxun Fang, Qiuxia Wu, Wenxiong Kang in their work, Strong feature representation ability was proven by CNN which needs huge training samples. The methods for verification of finger veins have been improved for better accuracy. As the database of finger vein available is very small, this was overcome by training two-channel network through an exquisite topological structure. The system integrates the original image information and mini region of interest and the verification was accomplished by final selected network system.

[4] Cihui Xie, Ajay Kumar in their work of Biometrics for person identification is done using vascular structures extracted from the images of finger vein, which produces the highly appropriate results. This is obtained by the use of convolutional neural networks with supervised discrete hashing technique. The results of the experiment state that, the proposed system achieves the better performing results over the other architectures of CNN. Improvement in performance is done by using the Region of Interest of finger vein and enhancing the features of vascular along with the background attenuation.

[5] Qing Chen, Lu Yang, Gongping Yang, Yilong Yin in their work, the performance of recognition of the finger vein gets degraded by deformation of image. To overcome this, extraction of feature like deformation-robust for matching methods is proposed to overcome this by detecting the deformation image correcting in the stage of preprocessing. A GADC method was proposed to detectthe deformable finger vein.

[6] Jinfeng Yang, Jianze Wei, Yihua Shi, in their work, as FV is growing very fast for the person identification/recognition, has led to the real application in biometrics. The practical problem is the huge database for FV recognition along with the FV ROI and enhancement of venous region has degraded the performance of FV biometric system. A novel approach has been presented for the extraction and enhancement of FV ROI and a model of HHsM using GrC is developed.

[7] S. N. Sravani, et. al., in their work Identification of veins and detection is main necessary for many clinical techniques on veins, like intravenous application and venepuncture along with the diagnosis of vascular diseases. For this, a portable vein imaging system is necessary which costs high for which a new cost competent portable imaging system of vein was proposed to locate the internal vein. Using NIR LED's which

uses 880nm wavelength an IR camera has been fabricated which deliver better contrast images than compared to other LED's at that wavelength.

3 Methods and Results

[1] An extraction of feature of vein network was done with a lighting system using 100's ofinfrared LED's. Using the database of the previous work and testing with altering diffusion constant and repeating it until getting the efficient results. With the new features like NCUT benchmark, SAB'11 and SAB'13 the physiological features of hand veins are extracted than the previous work (Figs. 1 and 2).

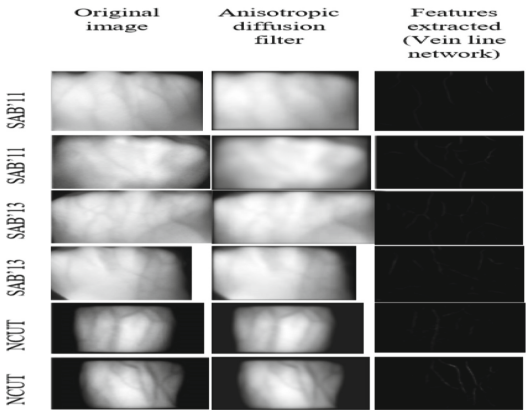

Fig. 1. Dorsal Database of three hand vein database

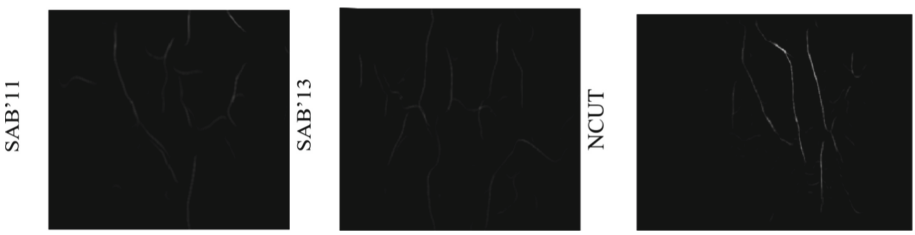

Fig. 2. Anisotropic diffusion filtered image

[2] A method was proposed for finding the effectiveness and robustness for the finger vein was carried out on the contact and contactless database. A comparison study was done with the proposed system and different feature extractions methods like maximum, mean, difference curvature, LBP, and sift have provided promising results. Also Gabor filters of robust and ISMO have been applied for the extraction of pattern of finger vein to be more insight with the verification of pattern of finger vein.

Two set of database were created by two universities, in which the database 1 was created with 3132 images from156 subjects at different intervals, and database 2 consists

of 680 images from 85 subjects, which are further processed for the parameter determination. Figure 5(a) and (b) illustrates the images of preprocessing from dataset 1 and (c) and (d) are the images of normalized from dataset 2 (Fig. 3).

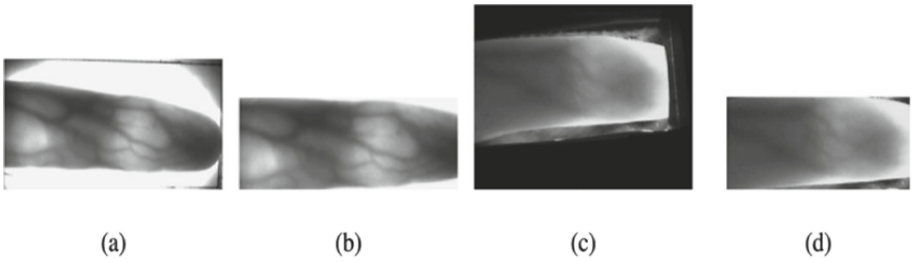

Fig. 3. Normalized results: (a) original 1; (b) gray normalized of (a); (c) original 2; (d) gray normalized of (c).

In the parameter detection section, the size of the neighbourhood and the size of the patch are determined. If the size of the neighbourhood is small, more the detailed patterns of veins are extracted with noise and if the size of the neighbourhood is large, features of veins are supressed by which smooth vein feature is extracted which may cause mismatch error. The size of the neighbourhood is found appropriately using the dataset for validation which consists of 612 images from 51 subjects from the remaining 51 subjects in database 1.

[3] Using MATLAB, with the mid-range system configuration, innermost edges of ROI is extracted from the SDUMLA database during the preprocessing using a network. The output of the network will be fed as input for the SVM classifier whose output will be averaged from the test samples of image pairs. The network is proposed that can extract the feature of the finger vein very effectively from the image. Hence the proposed network can be used for the processing for different images like Palm print, finger print and palm vein for the identification of authentication using these biometric modes.

The experimental configuration was setup and the different architectures were tested i.e. Two Channel Network, Two Stream Network, Joint Network whose performance were tested and compared.

The performance of the first architecture on the two database with its different types of selection of mini Region Of Interest methods are showed in the Table 1, which reflects the ability of the Two-channel network to represent the features.

The performance of the second architecture on the MMCBNU and SDUMLA databases and time taken to match was evaluated. The comparison of the performance and the Table 2 is comparison between Two-Channel and Two-Stream network.

The result reflects that with the proper mini-ROI, the two-stream network improves the system as the difference between the intra-class and the inter-class are extended calculatingly. As the two-stream network types cannot accomplish this goal self-reliantly on the diverse database, the join network system was proposed.

The performance of the join network system was evaluated by testing the four join network systems simultaneously for evaluation. The structure in the figure shows the

Table 1. The performance of the two-channel network.

The performance of the two-channel network		
Network	EER%	
	MMCBNU	SDUMLA
Two-channel	**0.20**	**0.94**
Two-channel-entr	1	3.62
Two-channel-corr	0.47	1.42
Two-channel-cent	0.30	1.89

Table 2. The performance of the two-channel network.

The performance of the two-channel network			
Network	EER%		Average matching time*
	MMCBNU	SDUMLA	
Two-channel	**0.20**	**0.94**	**0 + 50 ms**
Two-channel-entr	1	3.62	19 + 90 ms
Two-channel-corr	0.47	1.42	81 + 90 ms
Two-channel-cent	0.30	1.89	< 1 + 90 ms

*The average matching time includes the mini-ROI extraction, the 5-time forward calculation and the SVM prediction

two-channel along with its types and those other three systems are same. Table 1 reflects the proposed system performance summary on equal error rate and average matching time (Fig. 4; Table 3).

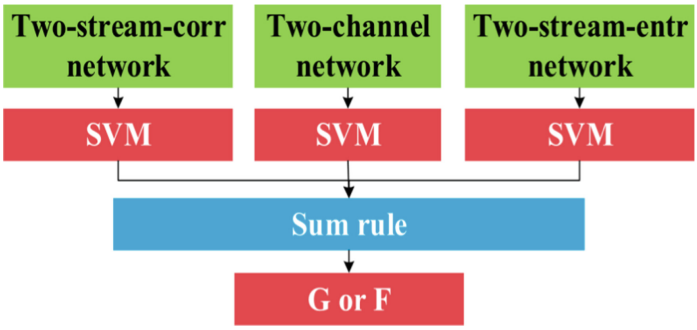

Fig. 4. Framework of Four Simple Joint Network System

[4] Using CNN architecture, matching of finger vein performance is studied. Using deep learning, system is trained to detect automatically through the learned features of

Table 3. Performance of the joint network system (entr and corr are abbreviations for the two-stream networks).

Performance of the joint network system (entr and corr are abbreviations for the two-stream networks)			
Network	EER (%)		Average matching time
	MMCBNU	SDUMLA	
Two-channel	0.20	0.94	0 + 50 ms
Two-stream-entr	0.13	1.26	19 + 90 ms
Two-stream-corr	0.30	0.47	81 + 90 ms
entr + corr	0.13	0.63	100 + 180 ms
Two-channel + entr	0.10	0.63	19 + 140 ms
Two-channel + corr	0.13	0.94	81 + 140 ms
Two-channel + entr + corr	0.13	0.63	100 + 230 ms
Selective network ' >'	0.10	0.47	50 + 90 ms
Selective network ' <'	0.27	0.47	50 + 90 ms

surface vascular network using the images of ROI and enhanced images. The experimental results state that MVGG-16 performs better than LCNN, which takes more time to train which produce the better match scores. Through many iterative through the network, determine the pair of finger vein images. It was concluded that there is improvement in the performance using ROI images of finger vein with enhanced feature of vascular and attenuation of background improves the performance significantly (Figs. 5–7).

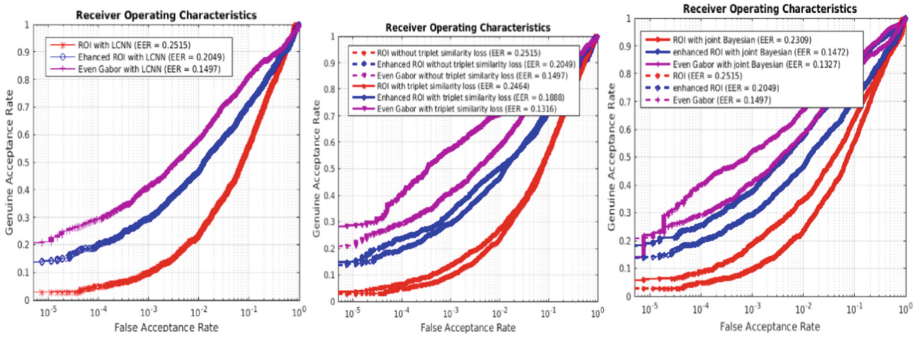

(a) (b) (c)

Fig. 5. (a) Using LCNN ROC performance comparison, (b) using triplet similarity loss ROC performance comparison and (c) ROC with Bayesian approach using LCNN.

Figure 5 (i) illustrates the matching performance of the respective ROC enhanced images is superior to the images of ROI. The ROI image enhancement with the use of

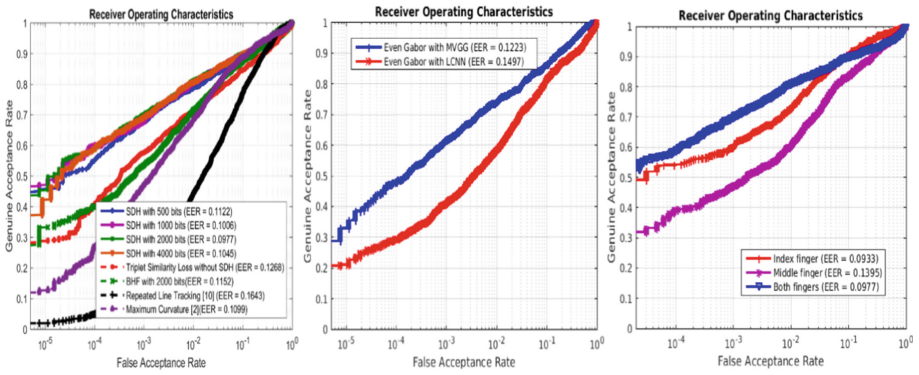

(a) (b) (c)

Fig. 6. (a) ROC with SDH and previous work using triplet loss based LCNN, (b) performance of ROC using modified VGG-16 and (c) ROC performance using the finger vein images from a single finger.

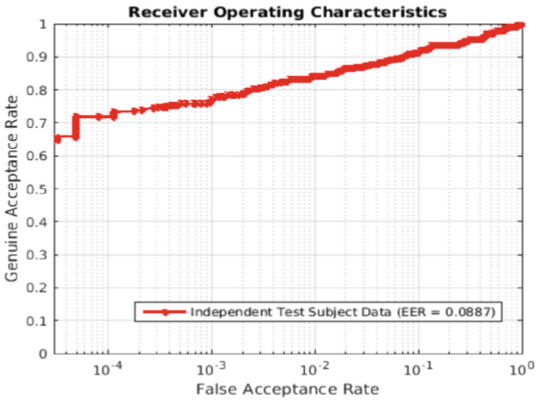

Fig. 7. The performance of matching finger-vein images using independent test subjects.

Gabor filter supress the noisy pixels significantly and vascular region will be emphasised which is the reason for the accuracy. (ii) Illustrate the results of trained Siamese triplet using LCNN with similarity loss function architecture which provides higher performance results than LCNN. LCNN tries to matches label of its samples where the LCNN along with the similarity loss prominences on resemblances between the images, which is the reason for the higher performance of ROC. (iii) Illustrates the results of ROC using the classification scheme joint Bayesian along with LCNN which shows the improvement in the performance over the LCNN.

Figure 6 (i) Illustrate the comparison of the use of SDH scheme and LCNN with triplet loss function used with supervised discrete hashing. It also illustrates the ROC of the tests images and using repeated line tracking matching protocol with maximum curvature. Using LCNN and SDH offers better performance and also reduces the template size. ii)

Illustrate the results of modified VGG-16 a CNN architecture which prohibits the use of SDH scheme to gather feature generating single match score. We can summarize from the ROC's that the matching of the finger-vein images performance is high using VGG-16 architecture than the trained LCNN. Iii) Illustrates the comparison of performance of SDH using finger vein image and ROC using triplet loss LCNN data sets of index finger and the middle finger. The results reflect that the performance using both fingers is better than using the single and index finger and also better that of the performance using middle finger, and Fig. 7 illustrates the performance of the matching of finger vein with the self-learned feature of ROC of finger vein data of independent test subjects.

[5] To deal with the deformation in the images of finger vein, an GADC method is proposed, which corrects the deformation in image by first detecting the deformation in the image of finger vein. GADC consists of two types of transformation, i.e. linear and non-linear. The outline of the framework is as shown in the figure below (Fig. 8).

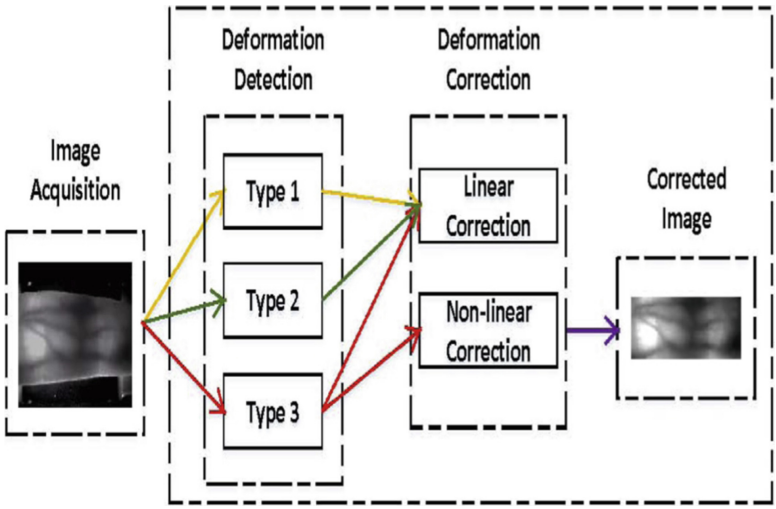

Fig. 8. GADC method block diagram.

The deformation of the finger vein is detected by the six sub steps. At first, the boundary of the finger is obtained by the method of boundary detection called superpixel. Later, on the boundaries, line fitting is done by fitting the upper boundary values on the Lupper line and the lower boundary values on the Llower line respectively, whose co-efficient of slope is represented by γupper and γlower. Calculation of one of the parameter i.e. the widths named as djoint1, djoint2 and dfinger root, by detecting the distal and proximal inter-phalangeal joints using sliding window. The angle amid the two straight lines can be measured by fitting the boundaries, i.e. αupp_joint1, αdown_joint1. The deformation of the image in type1, type2 and type3 is detected and it is corrected based on the values of rth_low1, rth_upp1, εth, αupp_joint1, αdown_joint1 taken.

The step in the algorithm is shown below. The measurement of the finger vein from its image is illustrated below (Fig. 9).

Algorithm 1
Detection of finger vein deformation.

INPUT: Original image I
OUTPUT: Deformation vector $\boldsymbol{D}$, finger boundary image $I_{boundary}$.
1. *(1) Finger edge detection;*
2. *(2) Line fitting of the points on finger boundaries;*
3. *(3) Detection of the phalangeal joints and calculation of the related parameters;*
4. *(4) Detection of the image deformation in type 1;*
5. *if* $t_{1low} < r_{joints} < t_{1up}$ & $|\gamma_{lower}| + |\gamma_{upper}| < t_{1angle}$ *then*
6. $D\{1\}=0$;
7. *else*
8. $D\{1\}=d_{finger\,root}$;
9. *end*
10. *(5) Detection of the image deformation in type 2;*
11. *if* $(t_{2low1} < \alpha_{upp\_joint1} < t_{2up1})$ & $(t_{2low1} < \alpha_{down\_joint1} < t_{2up1})$& $(t_{2low2} < r_{root-joint1} < t_{2up2})$ *then*
12. $D\{2\}=0$;
13. *else*
14. $D\{2\}=d_{finger\,root}$;
15. *end*
16. *(6) Detection of the image deformation in type 3;*
17. *if* $|\alpha_{upp\_joint1} - \alpha_{down\_joint1}| < t_{3rotate}$ *then*
18. $D\{3\}=0$;
19. *else*
20. $D\{3\}=\frac{\alpha_{upp\_joint1}-\alpha_{down\_joint1}}{|\alpha_{upp\_joint1}-\alpha_{down\_joint1}|} d_{finger\ root}$;
21. *end*

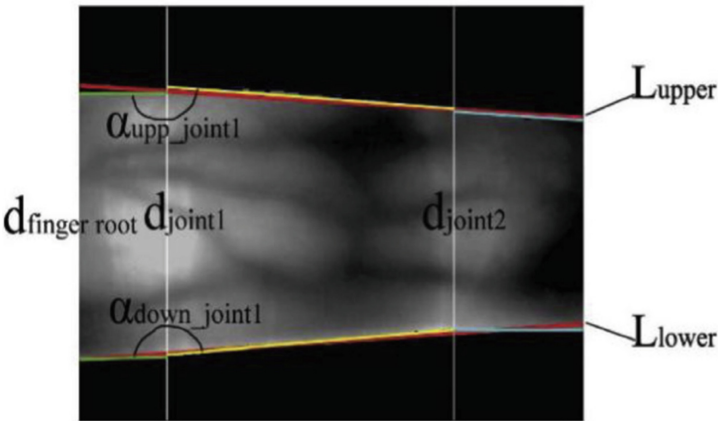

Fig. 9. The illustration of measurement of the finger in finger vein image.

The deformation correction using linear method consists of six substeps, finger width estimation on proximal inter-phalangeal joints, distal inter-phalangeal joints, finger width estimation between the proximal inter-phalangeal joints and the roots of the finger, finger width estimation between the proximal and distal inter-phalangeal joints, finger width estimation between the fingertip and the distal inter-phalangeal joints and

correction by using the method of bilinear interpolation. The steps used in the algorithm for correction is summarised as below (Figs. 10 and 11).

Correction of finger vein deformation.

INPUT: Deformation vector $\boldsymbol{D}$, finger boundary image $I_{boundary}$
OUTPUT: Finger vein image with correction I_{corr}.

for $i = 1$ *to* 3 *do*
  if $D\{i\} \neq 0$ *then*
    Estimate the widths of the finger on the phalangeal joints based $D\{i\}$;
    Estimate the widths of the finger h_i *between the finger root and the fingertip;*
    Correct using the bilinear interpolation method;
    for each column of the image do
      Compute the height h_{curr} *of the current column;*
      if $h_{curr} \neq h_i$ *then*
        The current column vector $H_{curr(x \times 1)}$ *is interpolated to the column vector* $H_{i(n \times 1)}$ *using bilinear interpolation method;*
      end
    end
  end
end
Obtain I_{corr} *composed of* H_i;
if $D\{3\} \neq 0$ *then*
  Correct using Ellipse Cross-sections Sampling Method in I_{corr};
end

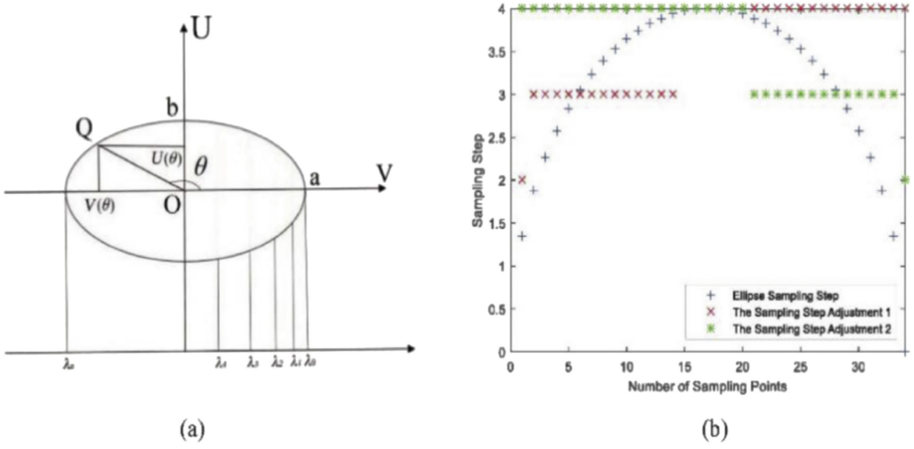

Fig. 10. (a) Ellipse of the cross-section; (b) Sampling step of ECS.

The ECS method is used for the deformation correction in type3 which is a non-linear method of transformation. Figure 10 illustrates the different steps like sampling of the image in which the sampling step is calculated, the adjustment of the sampling step, sampling and then normalization which are as shown in Fig. 11.

[6] The performance testing is done on the 5000 samples images collected from the 500 people, each providing 10 images which are 8-bit gray images. Out of 10, seven images are used to train the HHsM construction which is of 3500 FV images and three images out of 10 will be used for verification which is of 1500 FV images.

HHsm recognition curve of two layers and computational cost curve is illustrated in Figs. 12 and 13 respectively.

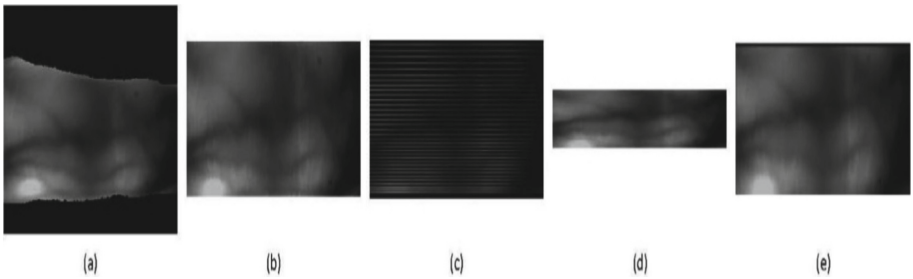

Fig. 11. Result of ECS model on SDUD database. (a) original finger vein image; (b) linear method corrected image; (c) sampling rows; (d) sampled image; and (e) normalized images

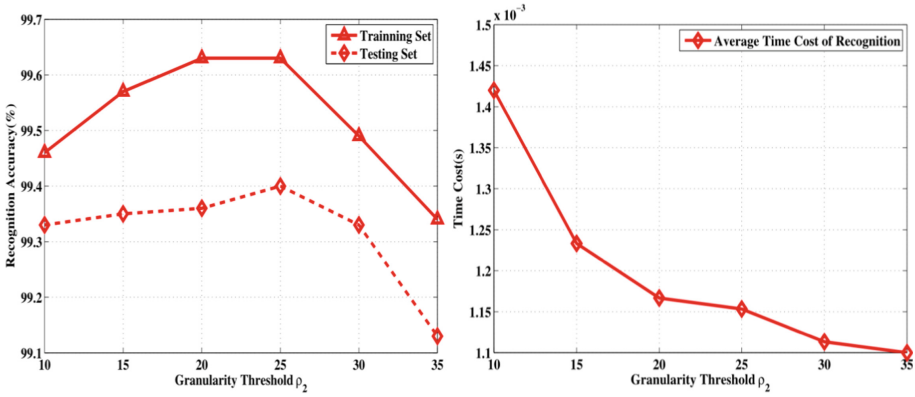

Fig. 12. (a) Accuracy curves of two-layer HHsMs. (b) The average time cost curve of HHsMs in FV recognition of two-layer

In Fig. 12(a) the solid line curve is the results of recognition using training set samples and the dashed line in the curve shows the results of recognition using samples from testing set.

Figure 12(a) and (b) the curves for computational cost and recognition accuracy is plotted respectively against ρ_2. (b) Shows that recognition efficiency increases with increasing ρ_2. HHsm recognition curve of three layers and average time cost curve is illustrated in Fig. 13(a) and (b).

The solid lines and the dashed line in the curve shows the results of recognition using samples from training set and testing set.

Figure 13(a) and (b) The curves for computational cost and recognition accuracy is plotted respectively against ρ3. Compared to Fig. 12, Fig. 13 shows the best accuracy of recognition with Fig. 12(a) and (b) The curves for computational cost and recognition accuracy is plotted respectively against ρ2. (b) Shows that recognition efficiency increases with increasing ρ3.

HHsm recognition curve of three layers and average time cost curve is illustrated in Figs. 14 and 15 respectively.

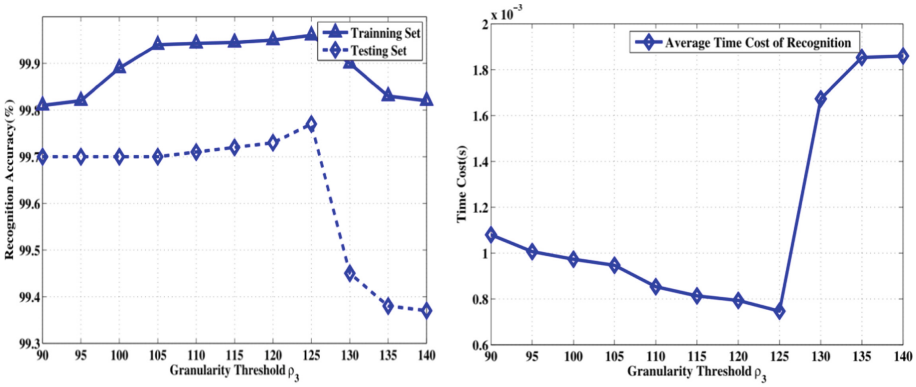

Fig. 13. (a) Accuracy curves of three-layer HHsM, (b) The time cost average curve of three-layer HHsM in FV recognition

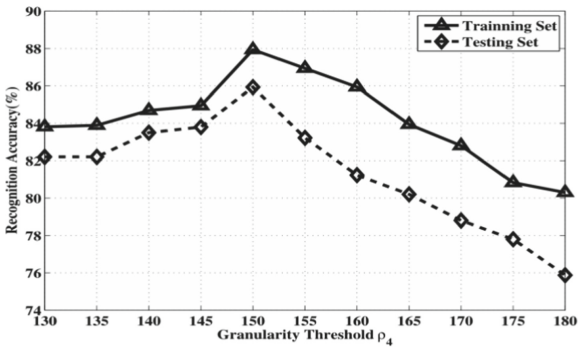

Fig. 14. Accuracy curves of four-layer HHsMs.

The solid lines and the dashed line in the curve shows the results of recognition using samples from training set and testing set.

For the evaluation of proposed HHsM is compared with the GrC method which is used in the recognition of hand written numeral, segmentation of image and retrieval of image. Table 4 reflects the accuracy and the time cost of the three methods i.e. SRM based, HsGC based and the proposed HHsM method. Hence it can be seen that the proposed method will be very useful in developing the new FV recognition system using GrC.

[7] OpenCV platform tool is used for real time application. Using OpenCV and program is written in C-language to process the videos of acquired veins through IR camera connected to PC using USB 2.0. At first the acquisition of video is done using near infrared LEDs which obtains the image by reflecting the light back from the targeted body. Here the frame rate is set to 15fps which results in processing the video faster. The next step is to process the image by enhancing the quality of the picture. Hence the image is converted to grayscale which gets processes faster with short time compared to that

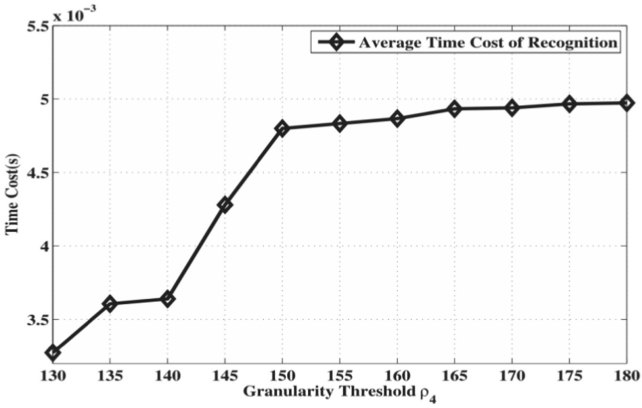

Fig. 15. The time cost average curve of HHsMs in FV recognition of four-layer.

Table 4. Comparisons of different GrC-based methods in FV recognition.

Methods	A-Rate (%)	T-Cost (s)
SRM-based [35]	98.54	9.30e − 3
HsGrC-based [64]	95.62	5.49e − 3
The proposed HHsM	99.78	7.47e − 4

of colored image. Also the entire process depends on setting of ROI plays a prime role on which the. The image contrast is enhanced; it is stretch beyond its assigned values as per the need. Discrepancy between the veins with its surrounds will be easier as the appearance of the slightly dark veins will be darker. After the stretching to the new scale, normalization will be done on the digital grayscale image.

As some images will be having darker region, there will be presence of some salt and pepper noise. As the images will be used for medical purpose, and the edges of veins should not get tampered, hence two median filters are used after the stretching of the contrast which will be displayed in the size of ROI in which the user can vary the contrast of the grayscale image to distinguish the surrounding skin and the veins. Segmentation is done for the image which is contrast stretched, to highlight veins from its background. The boundaries between pixels of the foreground and pixels of background will be cleared by the marks of the adaptive thresholding (Figs. 16–20).

The images below are the output of the above mentioned steps.

The Table 5 shows the results of T-test:

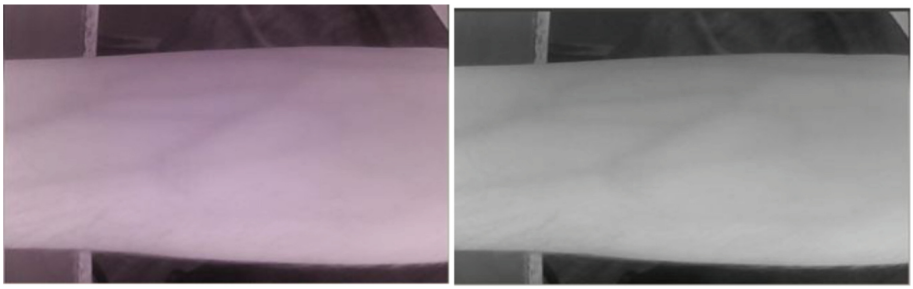

(a) (b)

Fig. 16. Acquired input frame Screenshot and Gray scale conversion Screenshot

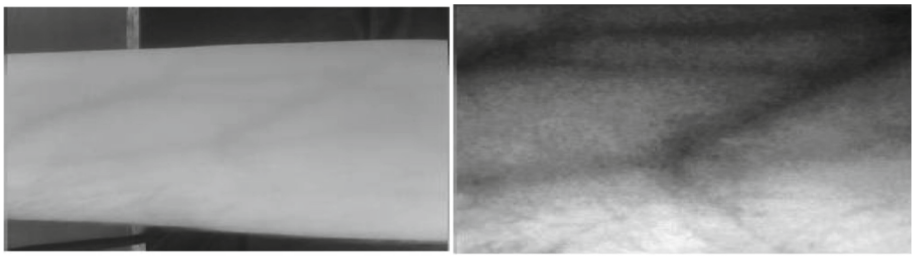

(a) (b)

Fig. 17. Gray image and Image with Contrast stretched within the ROI

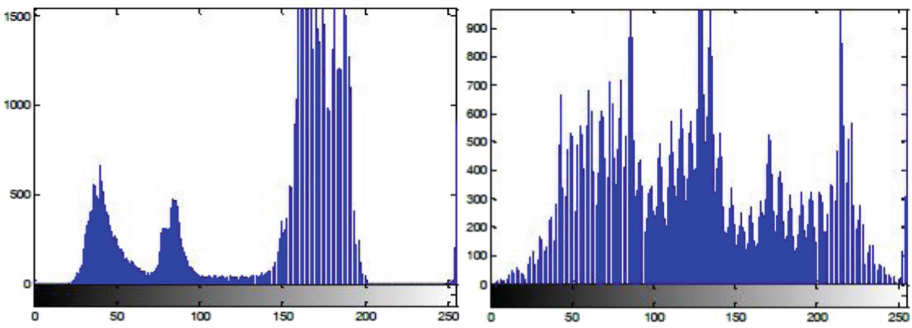

(a) (b)

Fig. 18. Histogram of gray scaled image and Contrast stretched Histogram ROI

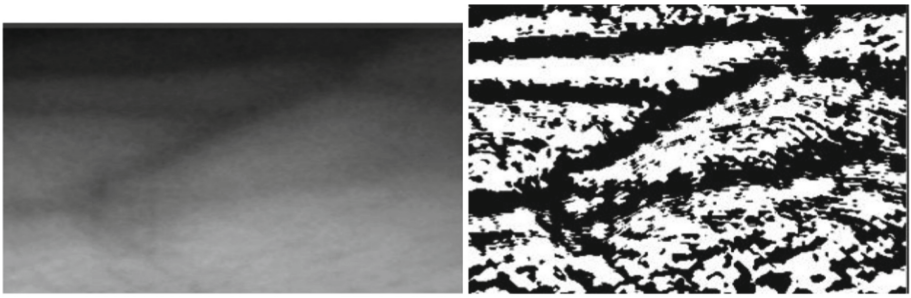

(a) (b)

Fig. 19. Contrast Enhancement Snapshot and Adaptive threshold in ROI

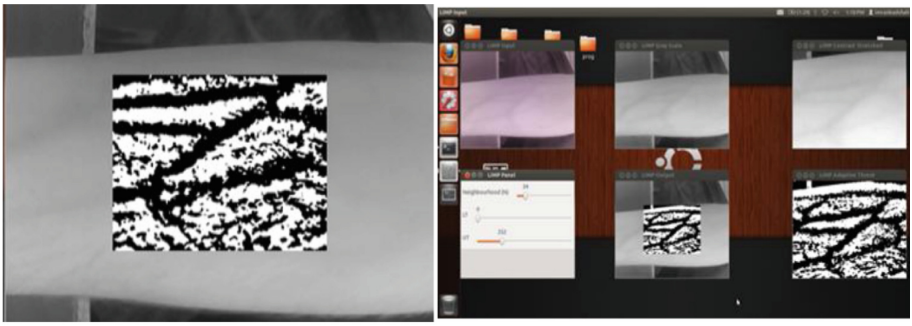

(a) (b)

Fig. 20. Frame of Grayscale with ROI and Screen preview of subject's vein

Table 5. Results of T-test

Sl. no	Parameter	Sig value
1	Gender	0.40
2	Age	0.000
3	Complexion	0.001
4	Gender and Age	0.850
5	Gender and Complexion	0.095
6	Age and Complexion	0.000

4 Conclusion

For authentication/biometric application, extraction of the vein patter is main feature for recognition.To extract the features from the vein network, we can use SAB'11, SAB'13 and NCUT benchmark. It can also be done by Radon transformation in Radon space which will be verified by the encoded images. Image deformation technique is used

for detection and correction using geometric of finger vein. Also using the linear and non-linear transformation method, image deformation will be accurately detected and corrected. The GWEF for extracting the ROI and enhances the images ridge information and the HHsM is very efficient in handling the recognition of finger vein problems.

By studying the listed works, for the authentication/biometric application using veins, there are different techniques for the extraction of ROI of the veins. Also, different methods to extract the features from the vein structure for better identification.

The work can be further extended for the capturing of vein structure with better quality images using different IR capturing system. Also the previous works opens the space for the researchers to do the research to extract the different features by studying the veins structure for better accuracy. Also the study of structure of veins can be used in medical applications to solve different nerve problems.

References

1. Hachemi Benziane, S., Benyettou, A.: Anisotropic diffusion filter for dorsal hand vein features extraction, IJBB, Vol. 1 (2016)
2. Qin, H.: He, X., Yao, X., Li, H.: Finger-vein verification based on the curvature in Radon space. Exp. Syst. Appl. **82** (2017) 151–161 , 0957–4174/© 2017 Elsevier
3. Fang, Y., Wu, Q., Kang, W.: A novel finger vein verification system based on two-stream convolutional network learning. Neurocomputing **290**, 100–107 (2018)
4. Xie, C., Kumar, A.: Finger vein identification using convolutional neural network and supervised discrete hashing. Patt. Recog. Lett. **119**, 148–156 (2019)
5. Chen, Q., Yang, L., Yang, G., Yin, Y.: Geometric shape analysis based finger vein deformation detection and correction. Neurocomputing **311**, 112–125 (2018)
6. Yang, J., Wei, J., Shi, Y.: Accurate ROI localization and hierarchical hyper-sphere model for finger-vein recognition. Neurocomputing **328**, 171–181 (2019)
7. S. N. Sravani, S. Zahra Naqvi, N. Sriraam, M. Mansoor, I. Badshah, M. Saleem, G. Kumaravelu, Portable subcutaneous vein imaging system. Int. J. Biomed. Clin. Eng. **2**(2), 11–22
8. Akrouf, S.: Une approche multimodale pour l'identification du locuteur. Doctoral dissertation (2014)
9. Draper, S. C., Khisti, A., Martinian, E., Vetro, A., Yedidia, J. S.: Using distributed source coding to secure fingerprint biometrics. In: Acoustics, Speech and Signal Processing, ICASSP 2007, IEEE International Conference on, Vol. 2, pp. II–129. IEEE (2007)
10. Wang, Y., Tan, T., and Jain, A. K.: Combining face and iris biometrics for identity verification. In Audio-and Video-Based Biometric Person Authentication, pp. 805–813. Springer Berlin, Heidelberg (2003)
11. Huang, B. N., Dai, Y. G., Li, R. F., Tang, D. R., and Li, W. X.: Finger-vein authentication based on wide line detector and pattern normalization. In 20th International Conference on Pattern Recognition (ICPR), pp. 1269–1272 (2010)
12. Kauba, C., Reissig, J., and Uhl, A.: Pre-processing cascades and fusion in finger vein recognition. In BIOSIG, pp. 87–98 (2014)
13. Kumar, A., Zhou, Y.B.: Human identification using finger images. IEEE Trans. Image Process. **21**, 2228–2244 (2012)
14. Dong, L., Yang, G., Yin, Y., Xi, X., Yang, L., Liu, F.: Finger vein verification with vein textons. Int. J. Pattern Recognit. **29**, 1556003 (2015)

15. Yang, L., Yang, G., Yin, Y., Zhou, L.: A Survey of Finger Vein Recognition. In: Sun, Z., Shan, S., Sang, H., Zhou, J., Wang, Y., Yuan, W. (eds.) CCBR 2014. LNCS, vol. 8833, pp. 234–243. Springer, Cham (2014). https://doi.org/10.1007/978-3-319-12484-1_26
16. Balakrishna, K., Rao, M.: Tomato plant leaves disease classification using KNN and PNN. Int. J. Comput. Vis. Image Process. **9**(1), 51–63 (2019). https://doi.org/10.4018/IJCVIP.2019010104
17. Miura, N., Nagasaka, A., Miyatake, T.: Extraction of finger-vein patterns using maximum curvature points in image profiles. In: Proceedings of IAPR Conf. Machine Vis. and Appl., May, Tsukuba Science City, pp. 347–350 (2005)
18. Miura, N., Nagasaka, A., Miyatake, T.: Extraction of finger-vein patterns using maximum curvature points in image profiles. In: Proc. IAPR Conf. Machine Vis. and Appl., Tsukuba Science City, pp. 347–350 (2005)
19. Wu, X., He, R., Sun Z., Tan, T.: A light CNN for deep face representation with noisy labels (2016)
20. J. Hashimoto: Finger vein authentication technology and its future. In: Proceedings of the Digest of Technical Papers, Symposium on VLSI Circuits, pp. 5–8. IEEE (2006)
21. Zharov, V.P., Ferguson, S., Eidt, J.F., Howard, P.C., Fink, L.M., Waner, M.: Infrared imaging of subcutaneous veins. Lasers Surg. Med. **34**(1), 56–61 (2004)
22. Liu, Z., Yin, Y., Wang, H., Song, S., Li, Q.: Finger vein recognition with manifold learning. J. Netw. Comput. Appl. **33**(3), 275–282 (2010)
23. Wu, J.D., Ye, S.H.: Driver identification using finger-vein patterns with radon transform and neural network. Expert Syst. Appl. **36**(3), 5793–5799 (2009)
24. Xi, X., Yang, G., Yin, Y., Yang, L.: Finger vein recognition based on the hyperinformation feature. Opt. Eng. **53**(1), 013108 (2014)
25. Qiu, S., Liu, Y., Zhou, Y., Huang, J., Nie, Y.: Finger-vein recognition based on dual-sliding window localization and pseudo-elliptical transformer. Expert Syst. Appl. **64**, 618–632 (2016)
26. Yang, J., Shi, Y., Jia, G.: Finger-vein image matching based on adaptive curve transformation. Patt. Recog. **66**, 34–43 (2017)
27. Qin, H., He, X., Yao, X., Li, H.: Finger-vein verification based on the curvature in radon space. Expert Syst. Appl. **82**, 151–161 (2017)
28. Xi, X., Yang, L., Yin, Y.: Learning discriminative binary codes for finger vein recognition. Pattern Recognit. **66**, 26–33 (2017)
29. Arici, T., Dikbas, S., Altunbasak, Y.: A histogram modification framework and its application for image contrast enhancement. IEEE Trans. Image Process. **18**(9), 1921–1935 (2009). https://doi.org/10.1109/TIP.2009.2021548
30. Mashaghi, A., Vach, P.J., Tans, S.J.: Noise reduction by signal combination in Fourier space applied to drift correction in optical tweezers. Rev. Sci. Instrum. **82**, 115103 (2011). https://doi.org/10.1063/1.3658825